European Journal of Mechanics A/Solids 32 (2012) 52–58

Contents lists available at SciVerse ScienceDirect

European Journal of Mechanics A/Solids

journal homepage: www.elsevier.com/locate/ejmsol

On cavitation instabilities with interacting voids

Viggo Tvergaard

Department of Mechanical Engineering, Solid Mechanics Technical University of Denmark, DK-2800 Kgs. Lyngby, Denmark

ARTICLE INFO

Article history:
Received 9 May 2011
Accepted 25 September 2011
Available online 4 October 2011

Keywords:
Void growth
Plasticity
Cavitation instability
Finite strains

ABSTRACT

When a single void grows in an elastic–plastic material a cavitation instability may occur, if the stress triaxiality is sufficiently high. The effect of neighbouring voids on such unstable cavity growth is studied here by comparing two different models. The first model considers a periodic array of voids, which allows for different rates of growth of two different types of voids. The second model considers a single discretely represented void embedded in a porous ductile material. It is shown that these two models represent very different interaction behaviour. According to the first model small voids so far apart that the radius of the plastic zone around each void is less than 1% of the current spacing between the voids, can still affect each others at the occurrence of a cavitation instability such that one void stops growing while the other grows in an unstable manner. On the other hand, the second model only accounts for effects of neighbouring voids that are inside the plastic zone surrounding the central void. The unit cell models analysed are axisymmetric, considering the full range of unstable stress states with the transverse true stress either larger than or smaller than the axial true stress.

1. Introduction

For a single small void in an elastic–plastic solid under pure hydrostatic tension a critical stress level has been found, at which the void grows without bound for a stationary overall strain (Bishop et al., 1945; Hill, 1950). This unstable void expansion is driven by the elastic energy stored in the surrounding material. It has been shown that such cavitation instabilities also occur under axisymmetric stress states (Huang et al., 1991; Tvergaard et al., 1992), when the stress triaxiality is so high that the stress level is very high relative to the yield stress. More recently Niordson and Tvergaard (2006) have studied size-effects on the phenomenon and Legarth and Tvergaard (2010) have analysed such instabilities in a 3D stress state with anisotropic plasticity. Also, in the context of nonlinear elasticity there has been much interest in cavitation instabilities (Ball, 1982; Horgan and Abeyaratne, 1986; Horgan and Polignone, 1995).

Experiments of Ashby et al. (1989) for a metal wire bridging a crack in a glass matrix have shown fracture by the growth of a single void to a diameter visible on the fracture surface, which approaches half the diameter of the metal wire. This has resulted in speculations on how this single void would interact with other voids present in the material. Tvergaard (1996) has used an axisymmetric cell model containing two independently growing voids to study their interaction at a cavitation instability. Subsequently, Tvergaard and Vadillo (2007) and Tvergaard (2008) have studied the interaction with neighbouring voids by analysing the possible cavitation instability of a void embedded in a porous ductile material. Other studies have focused on the effect of different size voids. Thus, Faleskog and Shih (1997) have proposed the mechanism that a small cylindrical void between two larger cylindrical voids may experience highly accelerated growth in the local stress fields enhanced by the stress concentrations around the larger voids. Tvergaard (1998) used the axisymmetric two-void model to study the growth of a very small spherical void surrounded by much larger spherical voids, and found that also the small spherical void shows accelerated growth due to the stress fields around the larger voids. This was confirmed in an analysis based on nonlocal plasticity (Tvergaard and Niordson, 2004), although this study emphasized that a high growth rate of a very small void is not realistic if the void radius is as small as the characteristic material length.

In the present paper the axisymmetric cell model with two independently growing voids (Tvergaard, 1996) is reconsidered.In a study of cavitation instabilities this model has the advantage that each type of void is completely surrounded by voids of the other type, so that interaction of different discretely represented voids is modelled. The analyses carried out here consider very small void volume fractions, as is important in relation to cavitation instabilities, and are also extended to cover the range where the transverse stresses exceed the axial tensile stress. For comparison, analyses using the model with a void embedded in

E-mail address: viggo@mek.dtu.dk.

0997-7538/$ – see front matter © 2011 Elsevier Masson SAS. All rights reserved.
doi:10.1016/j.euromechsol.2011.09.011

a porous ductile material (Tvergaard and Vadillo, 2007; Tvergaard, 2008) are carried out as well. It is shown that these two models represent quite different aspects of the instability problem.

2. Problem formulation

The *first micromechanical model* to be analysed here is an axisymmetric model for a material with a periodic array of voids (Fig. 1), where two types of voids can have different size and grow independently. In the axisymmetric model (Fig. 2), also used in (Tvergaard, 1996), the voids are initially spherical, with radii R_1 and R_2, and each void has the opposite type of void as its six nearest neighbours. In the real periodic pattern of voids (Fig. 1) the axisymmetric model is indicated by a hatched region in Fig. 1a and by dashed circles in Fig. 1b. Thus, the axis denoted by x^1 in Fig. 2 is vertical in Fig. 1a and is normal to Fig. 1b. The axisymmetric unit cell applied to analyse such a staggered periodic pattern was first used by Tvergaard (1990b) for a whisker reinforced metal matrix composite, and was subsequently used (Tvergaard, 1996) for the periodic array of voids considered here.

It is noted that a full 3D model with many tiny voids represented discretely would be ideal for investigating whether or not these voids would interact in a cavitation instability situation. However, this would be numerically very cumbersome. The axisymmetric two void model is chosen here, as it appears to be the simplest numerical model, which can give information about the interaction between initially spherical voids that grow independently.

For the square array seen on the cross-section (Fig. 1b) the approximation by an axisymmetric unit cell makes use of the initial radius $R_0 = B_0/\pi^{1/2}$ to keep the void volume fraction in the unit cell equal to that of the model material. When void No. 1 is that with initial radius R_1, the initial values of the void volume fractions for the two types of voids are

$$(f_1)_I = \frac{2}{3}\frac{R_1^3}{A_0 R_0^2}, \quad (f_2)_I = \frac{2}{3}\frac{R_2^3}{A_0 R_0^2} \tag{1}$$

In the cylindrical reference coordinate system used for the unit cell (Fig. 2), x^1 is the axial coordinate, x^2 is the radial coordinate and x^3 is the circumferential angle. The displacement components and the nominal traction components on reference base vectors are denoted by u^i and T^i. The symmetry boundary conditions at the ends of the cell are

$$u^1 = -U/2, \quad T^2 = 0 \quad \text{at } x^1 = 0 \tag{2}$$

$$u^1 = U/2, \quad T^2 = 0 \quad \text{at } x^1 = A_0 \tag{3}$$

where U is a constant. As the neighbouring cell is identical to the cell analysed but is rotated 180° so that its x^1 axis points in the opposite direction (see Fig. 1a), compatibility is approximately expressed by the requirements

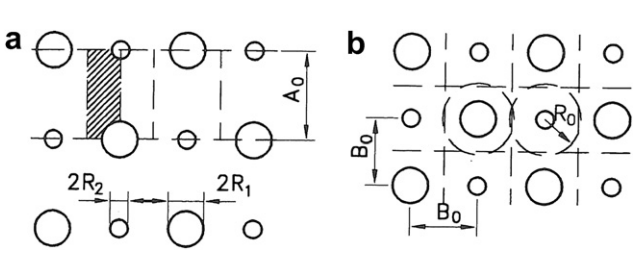

Fig. 1. Periodic staggered array of spherical voids with two different void sizes. (a) Cross-section along axial direction. (b) Cross-section normal to axial direction.

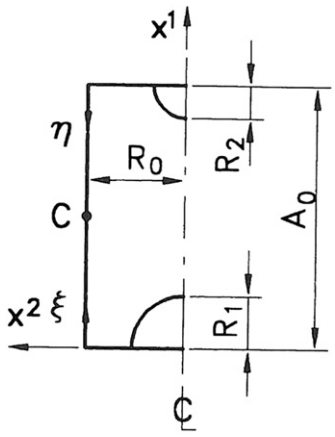

Fig. 2. Axisymmetric cell model used to analyse the staggered array of spherical voids, with x^1 along the axial direction.

$$u^1(\xi) = -u^1(\eta), \quad \text{for } \xi = \eta, \quad x^2 = R_0 \tag{4}$$

$$\left\{R_0 + u^2(\xi)\right\}^2 + \left\{R_0 + u^2(\eta)\right\}^2 = 2\left\{R_0 + u_C^2\right\}^2, \text{for} \xi = \eta, x^2 = R_0 \tag{5}$$

where ξ and η are distances from the bottom and the top of the cell, respectively, and u_C^2 is the radial displacement at the centre point C in Fig. 2. As has been explained at the first application of these boundary conditions to a metal matrix composite (Tvergaard, 1990b) Eq. (5) gives approximate compatibility between neighbouring cells in the axial direction, while Eq. (6) prescribes that the total cross-sectional area is independent of the x^1- coordinate, since such cross-sections consist of an equal number of cross-sections of the two types of neighbouring cells considered. In a subsequent paper Hom (1992) doing a full 3D analysis for a metal matrix composite found that this approximate cell model gives a good representation of the actual 3D results. The equilibrium conditions on the cell side are specified as

$$T^1(\xi) = T^1(\eta), \quad T^2(\xi) = T^2(\eta), \quad \text{for } \xi = \eta, x^2 = R_0 \tag{6}$$

The average logarithmic strains in the axial and transverse directions are $\varepsilon_1 = \ln(1 + U/A_0)$ and $\varepsilon_2 = \ln(1 + u_C^2/R_0)$, respectively.

The average nominal stresses are computed as the appropriate area averages of the microscopic nominal stress components on the surface, noting that it is necessary to average over both the cell analysed and one of the neighbouring cells of opposite kind. This gives axial and transverse nominal stress components, while all shear components vanish. The corresponding average true stresses S and T are calculated from the nominal stress values, using the average strains. In each increment, for a given increment $\dot{U}$ of the axial displacement, the increment $\dot{u}_C^2$ of the radial displacement at the centre is calculated such that the ratio of the average transverse stress T and the average axial stress S has the prescribed value

$$T/S = \rho \tag{7}$$

Finite strains are accounted for in the analyses, based on a convected coordinate Lagrangian formulation of the field equations, with the Cylindrical x^i coordinate system used as reference (see Fig. 2). Here, g_{ij} and G_{ij} are metric tensors in the reference configuration and the current configuration, respectively, with determinants g and G, and $\eta_{ij} = 1/2(G_{ij} - g_{ij})$ is the Lagrangian strain tensor. The contravariant components τ^{ij} of the Kirchhoff stress